

## Supporting Information

### The interplay between the supramolecular motifs of polypyridyl metal complexes and halogen bond networks in co-crystals.

Michael C. Pfrunder,<sup>a</sup> Aaron S. Micallef,<sup>\*,b</sup> Llewellyn Rintoul, Dennis P. Arnold,<sup>b</sup> and John McMurtrie<sup>\*,b</sup>

<sup>a</sup> University of Queensland, Brisbane, Queensland 4072, Australia. E-mail: [m.pfrunder@uq.edu.au](mailto:m.pfrunder@uq.edu.au)

<sup>b</sup> Queensland University of Technology (QUT), Brisbane, Queensland 4001, Australia. E-mail: [a.micallef@qut.edu.au](mailto:a.micallef@qut.edu.au), [l.rintoul@qut.edu.au](mailto:l.rintoul@qut.edu.au), [d.arnold@qut.edu.au](mailto:d.arnold@qut.edu.au), [j.mcmurtrie@qut.edu.au](mailto:j.mcmurtrie@qut.edu.au)

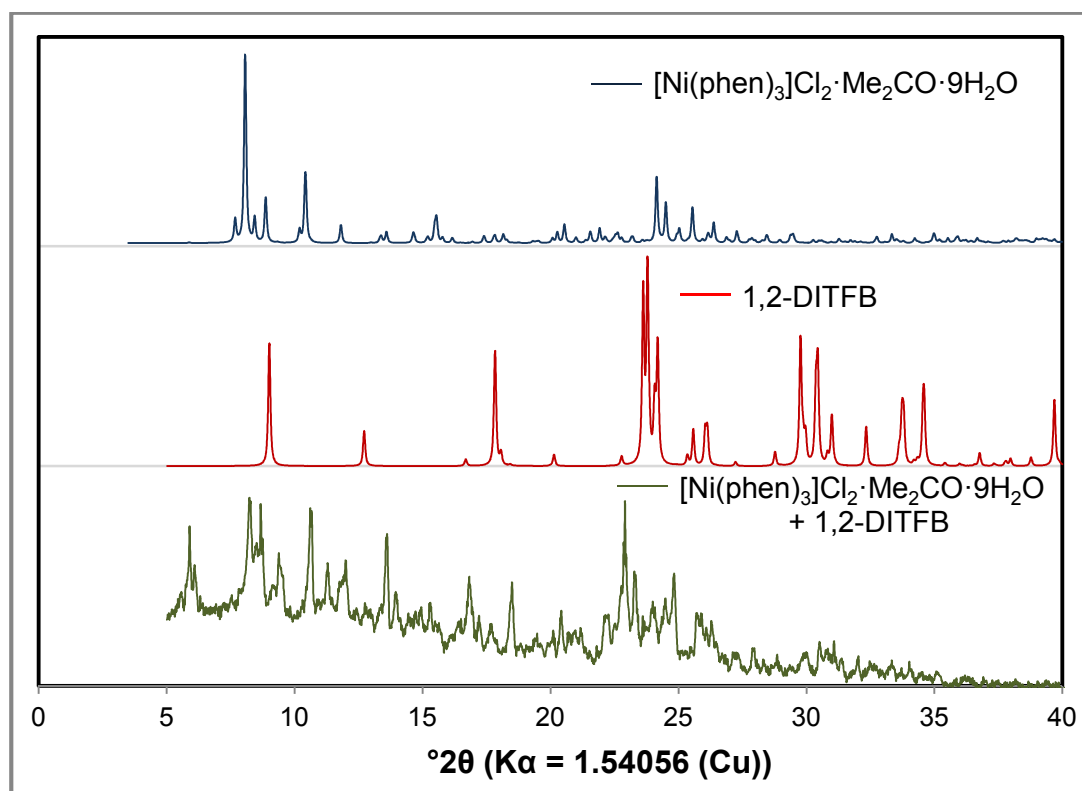


**Figure S1** PXRD pattern of material obtained through the attempted co-crystallisation of  $[\text{Ni}(\text{phen})_3]\text{Cl}_2 \cdot \text{H}_2\text{O}$  and 1,2-DITFB (green) compared with patterns of the individual starting components simulated from SCXRD data ( $[\text{Ni}(\text{phen})_3]\text{Cl}_2 \cdot \text{Me}_2\text{CO} \cdot 9\text{H}_2\text{O}$ : blue; 1,2-DITFB: red).

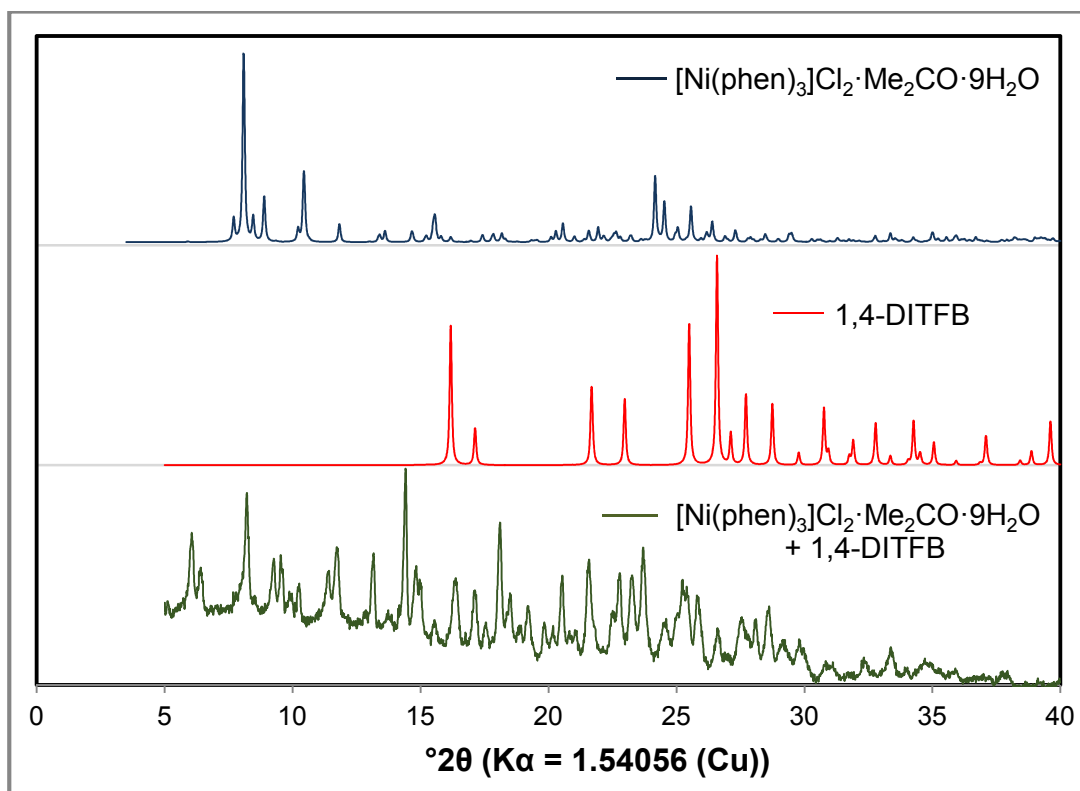


**Figure S2** PXRD pattern of material obtained through the attempted co-crystallisation of  $[\text{Ni}(\text{phen})_3]\text{Cl}_2 \cdot \text{H}_2\text{O}$  and 1,4-DITFB (green) compared with patterns of each of the individual starting components simulated from SCXRD data ( $[\text{Ni}(\text{phen})_3]\text{Cl}_2 \cdot \text{Me}_2\text{CO} \cdot 9\text{H}_2\text{O}$ : blue; 1,4-DITFB: red).

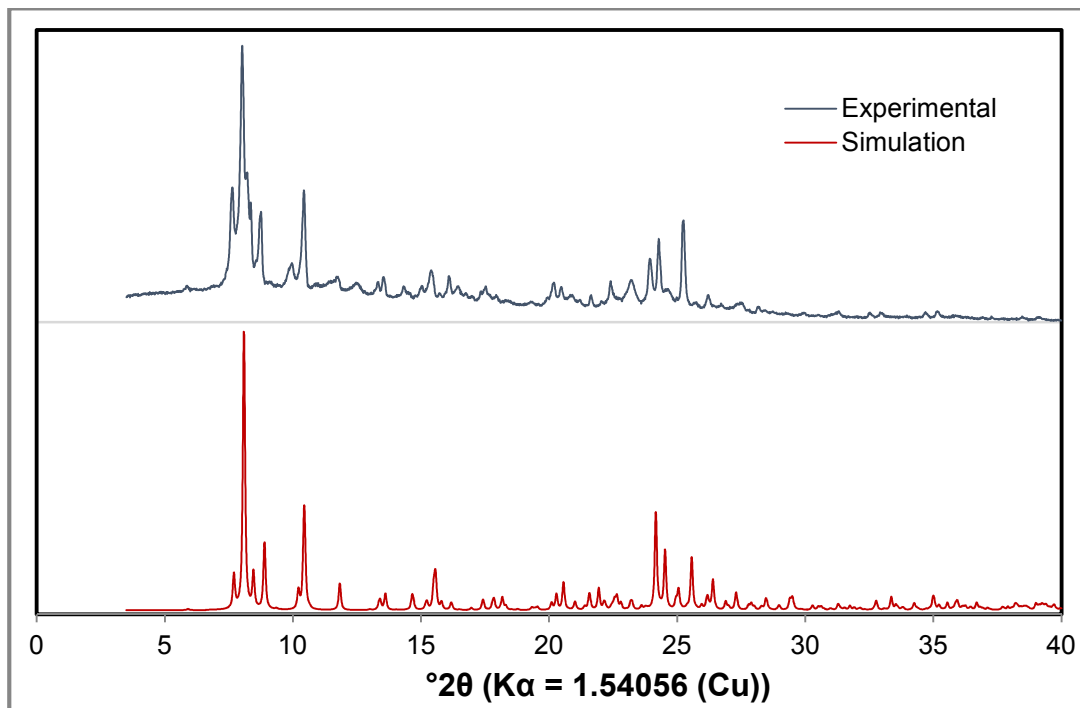


**Figure S3** PXRD pattern of  $[\text{Ni}(\text{phen})_3]\text{Cl}_2 \cdot \text{Me}_2\text{CO} \cdot 9\text{H}_2\text{O}$  (8; blue) compared to pattern simulated from SCXRD data (red).

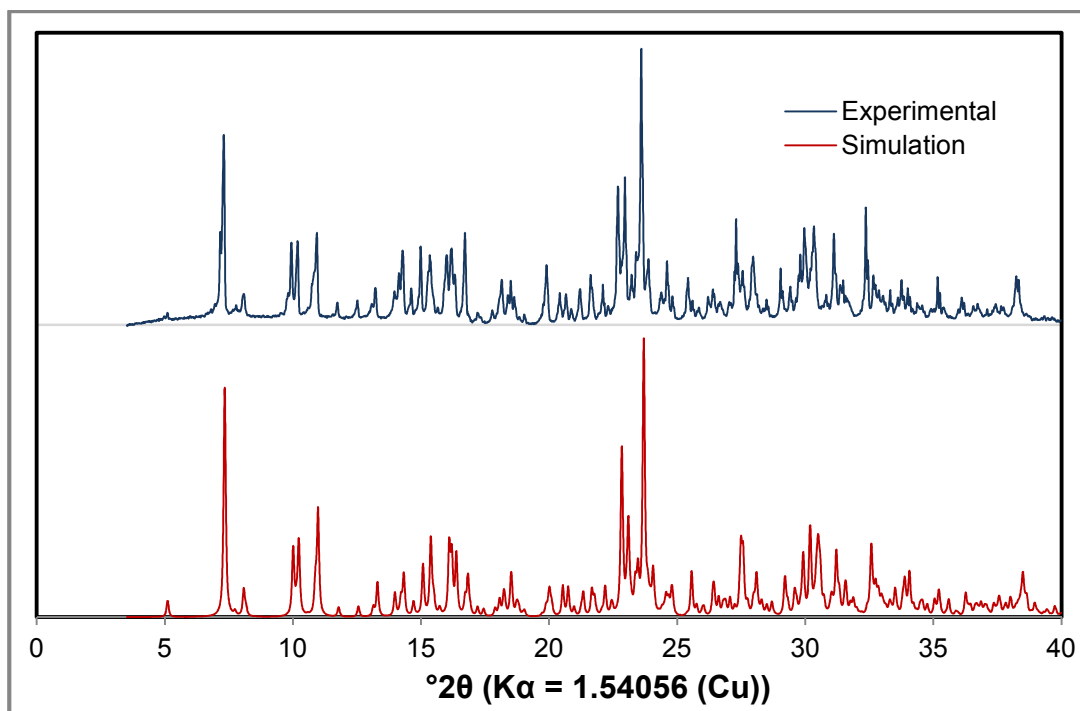


**Figure S4** PXRD pattern of  $[\text{Ni}(\text{phen})_3][(\text{1,2-DITFB})_2\text{I}_2] \cdot \text{MeOH}$  (**2**; blue) compared to pattern simulated from SCXRD data (red).

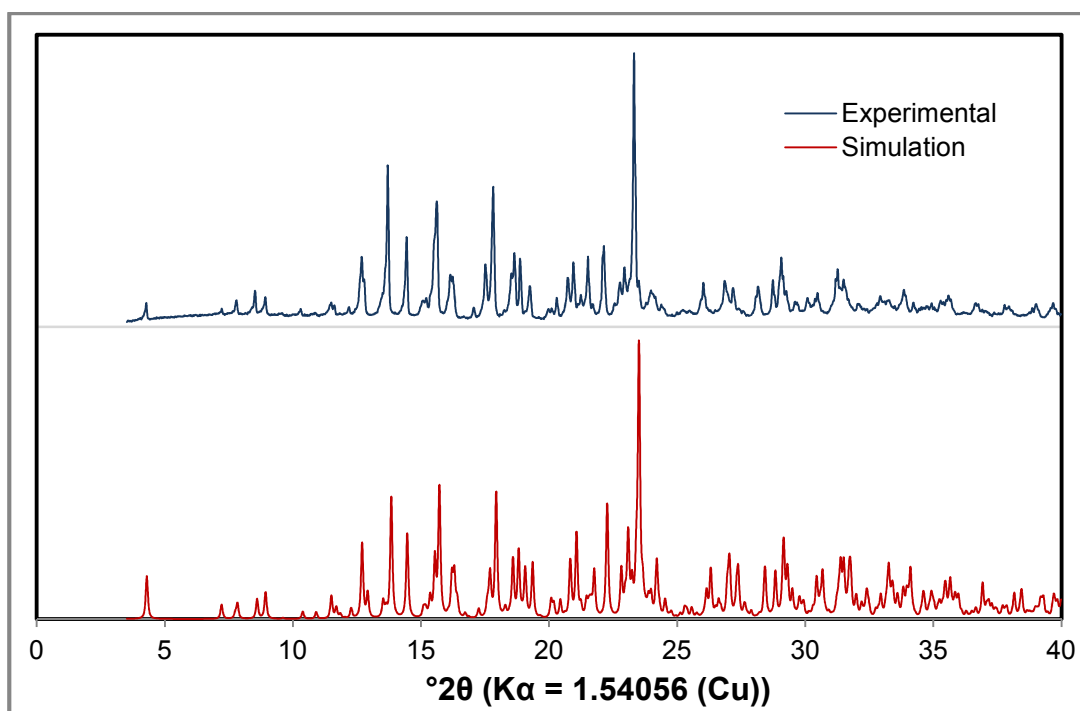


**Figure S5** PXRD pattern of  $[\text{Ni}(\text{phen})_3][(\text{1,3-DITFB})_3\text{I}_2]$  (**4**; blue) compared to pattern simulated from SCXRD data (red).

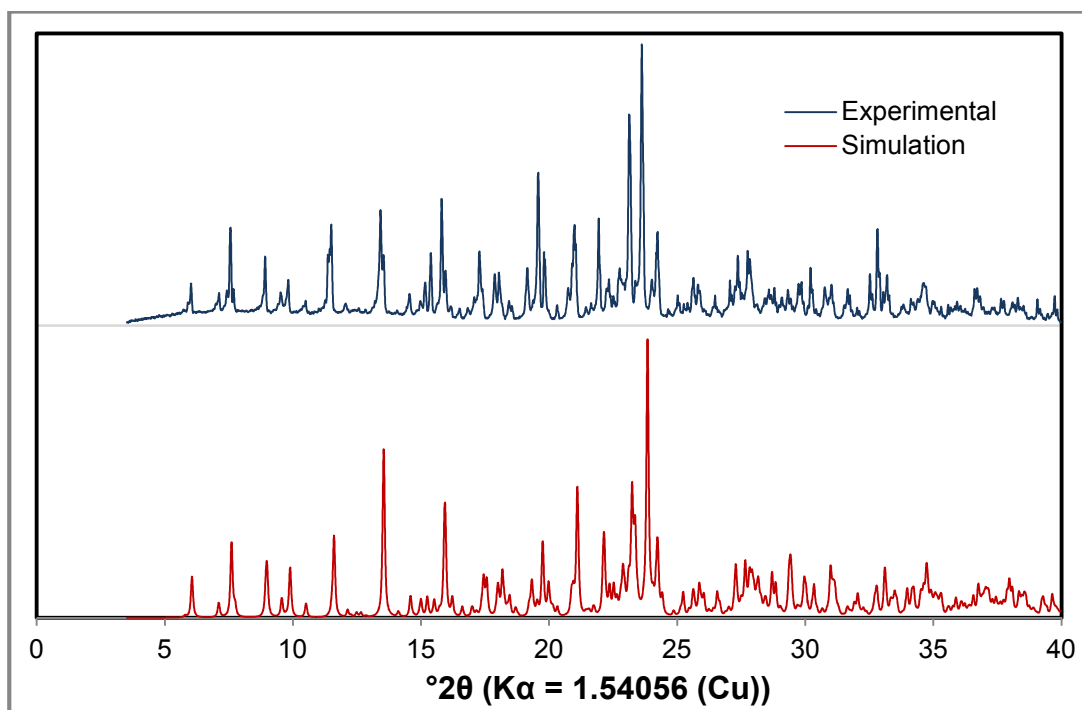


**Figure S6** PXRD pattern of  $[\text{Ni}(\text{phen})_3][(\text{1,4-DITFB})_3(\text{MeOH})_{0.5}\text{I}_2]$  (**1**; blue) compared to pattern simulated from SCXRD data (red).

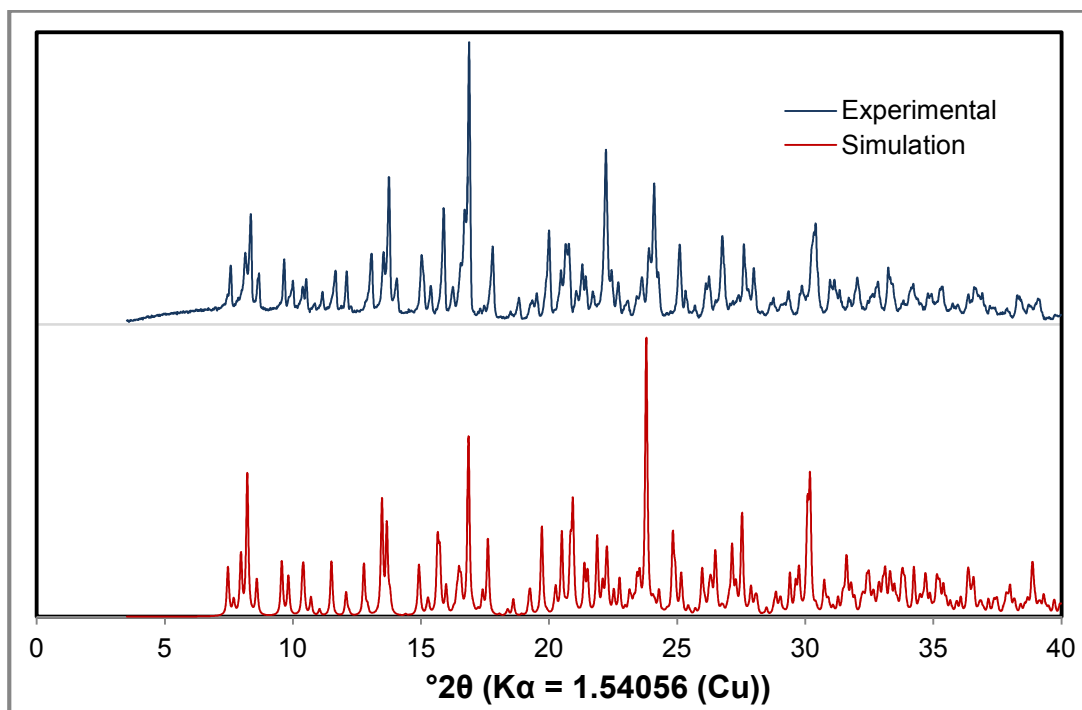


**Figure S7** PXRD pattern of  $[\text{Ni}(\text{phen})_3][(\text{1,3,5-TITFB})_2\text{I}_2] \cdot 0.5\text{MeOH} \cdot 1.5\text{H}_2\text{O}$  (**5**; blue) compared to pattern simulated from SCXRD data (red).

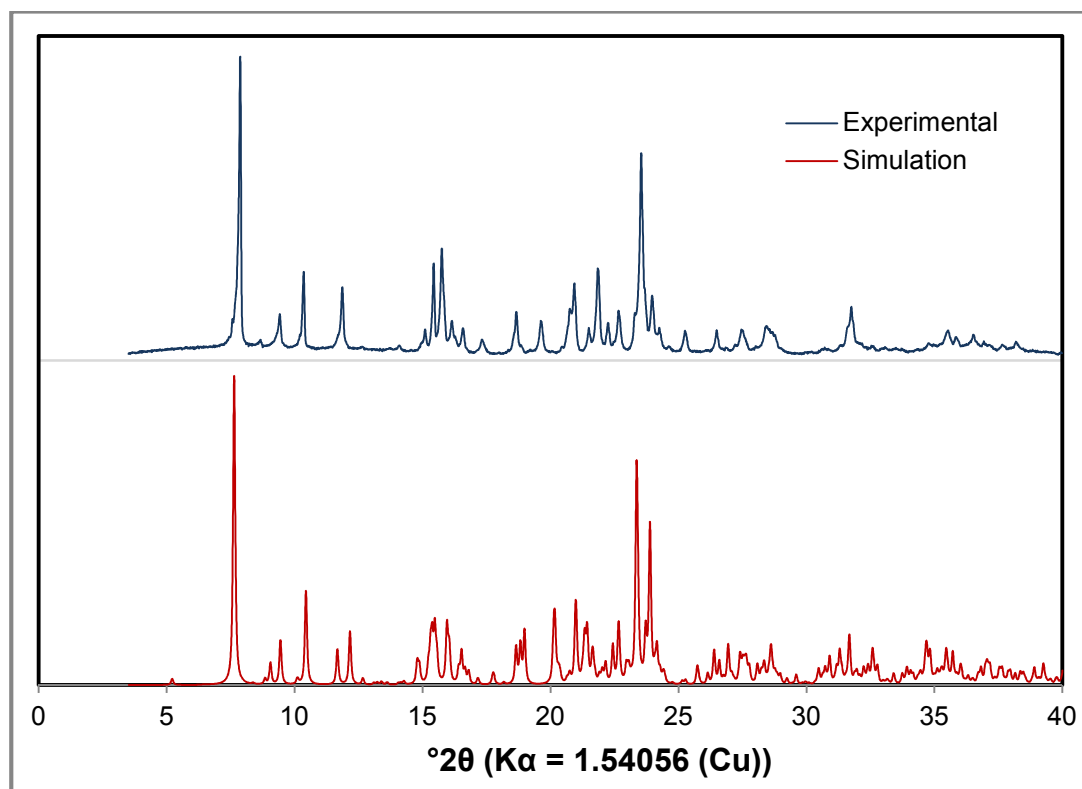


**Figure S8** PXRd pattern of  $[\text{Ni}(\text{phen})_3][(\text{1,3-DITFB})_2(\text{H}_2\text{O})_2\text{Cl}_2] \cdot 1.5\text{MeOH}$  (**6**; blue) collected at room temperature compared to pattern simulated from SCXRD data collected at 173K (red). The main peaks in the experimental pattern match those in the simulated pattern. The additional fine structure in the simulated pattern may arise as a consequence of the low temperature used to record the SCXRD data.